Grain growth in polycrystalline $Ba_{0,5}Sr_{0,5}TiO_3$ ceramics prepared at different sintering times

S. García , J. Portelles , F. Martínez, R. Font , J.R. Quiñones.
Facultad de Física-IMRE, Universidad de la Habana, San Lázaro y L, 10400, CUBA

J.M. Siqueiros
Centro de Ciencias de la Materia Condensada, Universidad Nacional Autónoma de México, Apartado Postal 2681, Ensenada, Baja California 22800, MÉXICO

Recibido el 7 de noviembre de 2001; aceptado el 22 de octubre de 2002

A grain size study based on the measurements of the maximum permittivity and the microstructure of samples of $Sr_{0,5}Ba_{0,5}TiO_3$ sintered at different time lengths at a fixed temperature is reported. A linear law of grain growth is found from the experimental results and properly described by the Johnson-Mehl-Avrami theory. The model predicts a zero nucleation rate.

Keywords: Grain size; sintering time; BST; dielectric permittivity

Se reportan los resultados de un estudio del comportamiento del tamaño de grano basado en medidas de permitividad dieléctrica máxima y en la microestructura de muestras de $Sr_{0,5}Ba_{0,5}TiO_3$ sinterizadas durante diferentes tiempos a temperatura fija. De los resultados experimentales se encuentra una ley lineal de crecimiento del grano con el tiempo de sinterizado descrita adecuadamente por la teoría de Johnson-Mehl-Avrami. El modelo predice una tasa cero de nucleación.

Descriptores: Tamaño de grano; tiempo de sinterizado; BST; permitividad dieléctrica.

PACS: 77.84.-s; 77.84.Dy; 81.35.+k; 81.40.-z

1. Introduction

In the last decade, a great deal of interest has evolved around ferroelectric thin films to be used in capacitors for integrated circuits and dynamic random access memories (DRAMs) among other applications [1-7]. Due to their high dielectric permittivity and low losses $Sr_{0,5}Ba_{0,5}TiO_3$ (BST50) ferroelectric ceramics are considered one of the most attractive materials for such kind of applications. On the other hand, miniaturization is a *sine qua non* requirement for capacitors to be used in present day electronics. For 256 Mbyte DRAM capacitors, for instance, film thickness must be less than 80 nm, imposing thus a strong requirement on the grain size of the films, additional to the good dielectric properties. The understanding the dependence of the dielectric properties with grain size and grain growth kinetics is, therefore, of great importance.

The effect of the sintering temperature and time in the ferroelectric properties of any ferroelectric ceramic and, in particular, the BST50 compound is well known [8-10]. These properties are closely related to crystallite size and therefore to the grain size obtained during the sintering process. By varying the sintering temperatures and times, heating rates, atmosphere composition and other parameters, grain size may be reasonably controlled [11-18].

In solid state phase transformation kinetics two cases may be distinguished: homogeneous and heterogeneous reactions. Among the latter, those where a nucleation and growth mechanism takes place are of special interest. Johnson, Mehl and Avrami [9] developed a theory that describes these processes predicting, within reasonable approximation individual nucleation measurements and growth rates. This theory has been successfully applied to biological processes, isothermal crystallization in glasses and metals [9], but as far as we know, it has not been applied to ferroelectric ceramics.

In this work a study of the grain size evolution as a function of sintering time in $Sr_{0,5}Ba_{0,5}TiO_3$ ceramics is presented. A law that governs the grain growth and the relation between grain size and the dielectric properties are established.

2. Experimental

The BST50 solid solution was prepared using the traditional ceramic technique [10] by mixing high purity $BaCO_3$, $SrCO_3$ and TiO_2 in an agate mortar for two hours. The resulting powders were calcined for 2 hours at 1000 °C and die pressed into 10 mm diameter, 2 mm thick tablets. Finally, the samples were sintered on a platinum foil in air at 1250 °C for 1, 2, 3, and 4 hours.

The density of the samples was determined by using the liquid displacement method and the measured values varied between 92 and 93% of the theoretical density. A good electrical contact was obtained using silver paste on both sides of the sample disks, fired at 700 °C for 1 hour.

A Phillips PW-1821 X-ray diffractometer with Cu ($\lambda_{k\alpha 1}$= 1,54056 Å $\lambda_{k\alpha 2}$= 1,54439 Å) anode was used to perform powder X-ray analysis of the crystalline structure of the samples at a 2^0/min scanning rate. A JGM-5300 scanning electron microscope (SEM) by JEOL was used for the grain analysis. The grain size was statistically determined from the SEM micrographs of the fractured samples.

Dielectric measurements were made at 1 kHz using an RLC (Tesla BM509) bridge coupled to a personal computer. The temperature dependence of the permittivity was determined by thermoelectric analysis in the -160 °C to 25 °C temperature range.

3. Results

Figure 1 shows the X-ray diffraction (XRD) spectra recorded at room temperature in the $20° < 2\theta < 90°$ range for BST50 samples sintered at 1250 °C for 1, 2, 3 and 4 hours. All the lines present correspond to the BST cubic phase and no additional lines in the powder patterns were detected. The lattice parameter obtained from the XRD patterns, a = 3.95 Å, agrees with previously reported values [11].

The microstructure of samples sintered at 1250 °C at different times from a) 1 hour to d) 4 hours is presented in the micrographs in Fig. 2. Well-defined grains uniform in size and shape are observed. Figure 3 condenses the statistical results for the average grain size for the different sintering times. The fitting performed to the experimental values with a correlation coefficient of 0.98, indicated a linear grain growth with the sintering time. The grain volume would then be proportional to t^3, (each dimension grows proportional to t) where t is the sintering time.

Measurements of the dielectric permittivity (ε) as a function of temperature were performed at 1 kHz, Fig. 4. Broad peaks corresponding to the para-ferroelectric transition at the temperature of maximum dielectric permittivity, T_{max}, as well as an increase in the permittivity values with grain size were observed. T_{max} remains fixed for the different grain sizes in good agreement with previously reported values [11]. In the curves corresponding to 2, 3 and 4 hours, in Fig. 4, three maxima of the dielectric permittivity are observed. The highest peak corresponds to the cubic-tetragonal phase transition. The peak at intermediate temperature to a tetragonal-orthorhombic and the one at the lower temperature to an orthorhombic-rhombohedric phase transitions. The growth of the grains at the expense of the grain boundaries is a viable explanation for the raise in the permittivity values with

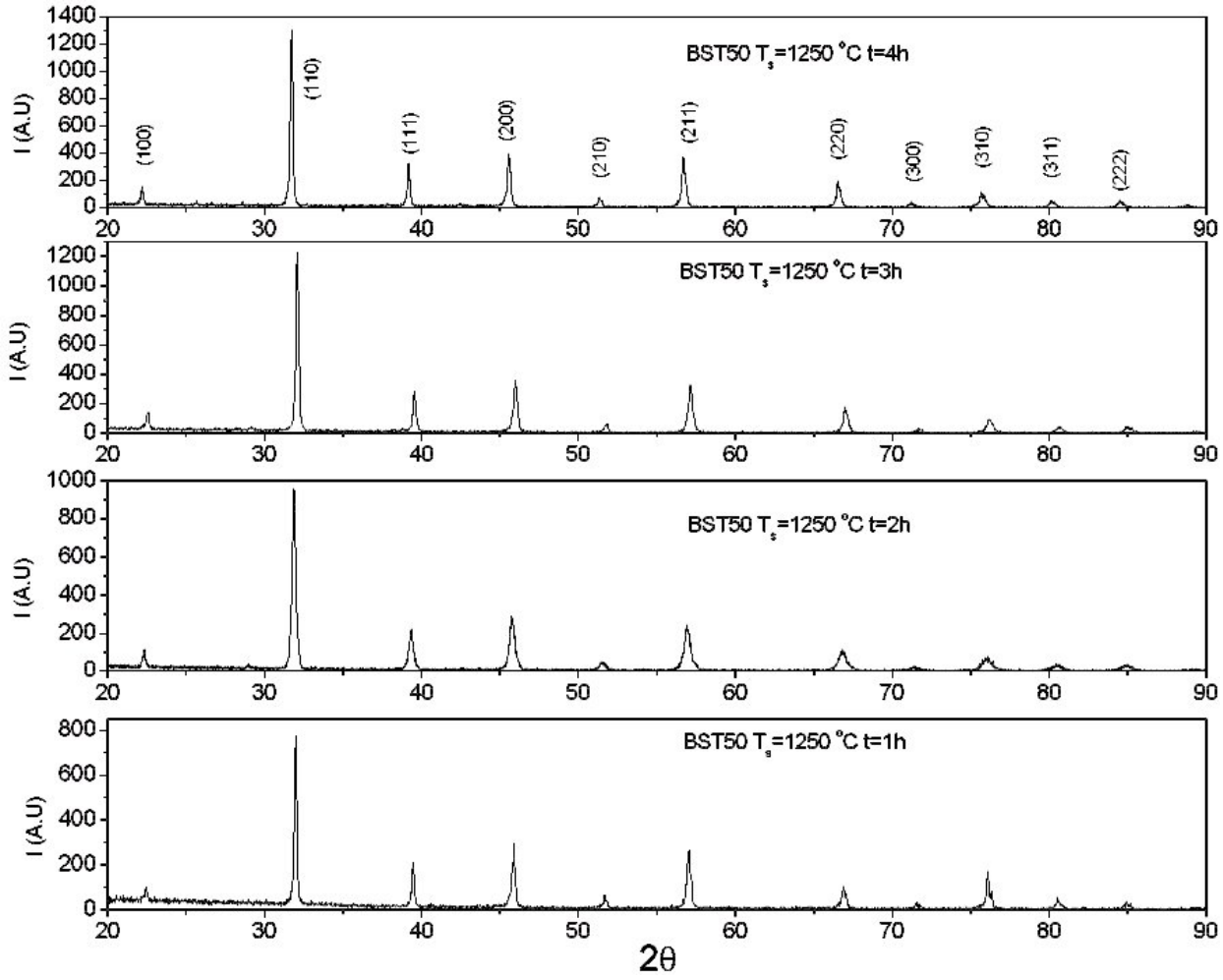

FIGURE 1. X-ray diffraction pattern of the BST50 samples sintered at 1250 ^{0}C for 1, 2, 3 and 4 hours.

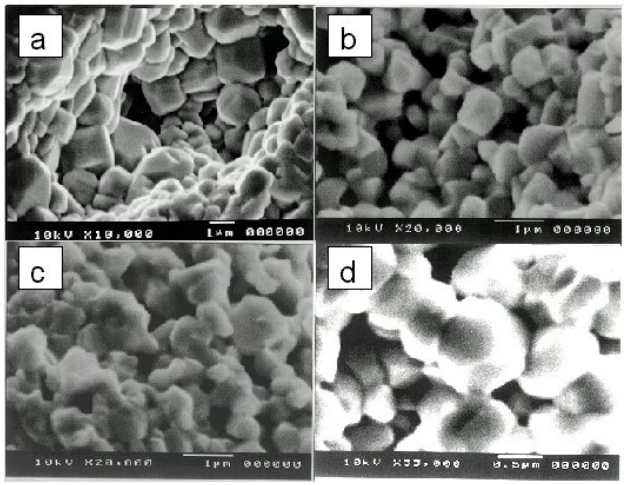

FIGURE 2. SEM micrographs of BST50 samples sintered at a) 1 h b) 2 h c) 3 h d) 4 h.

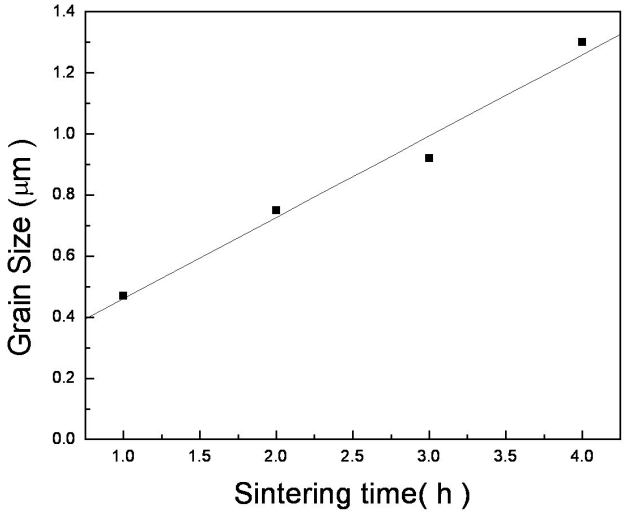

FIGURE 3. Average grain size of the BST50 samples as a function of sintering time.

sintering temperature since, as the grain boundaries diminish, so do the defects in that zone of the material. If we attribute a deteriorating effect on the permittivity to the defects, its reduction will lead to higher values of ε.

To properly consider the grain size effect on the dielectric properties of the material, its porosity must be taken into account. Therefore, to isolate the influence of the grain size on the dielectric permittivity its value (ε^*) in the absence of pores or voids was determined. For this purpose, Wiener's model [12] is applied and, in this case a minority phase of spherical pores embedded in a BST50 matrix of permittivity ε is considered. Taking into account that the porosity of the samples is less than 0.1 and the small value of the pore permittivity $\varepsilon^{**} \approx \varepsilon_0 << \varepsilon$, the mixing rule used by Wagner

$$\varepsilon - \varepsilon^*/\varepsilon + 2\varepsilon^* = V(\varepsilon^{**} - \varepsilon^*)/(\varepsilon^{**} + 2\varepsilon^*)$$

can be expressed as

$$\varepsilon^* = \varepsilon \quad \frac{1 + V/2}{1 - V}, \tag{1}$$

where ε^* is the measured value of the dielectric permittivity and V is the pore volume fraction. The relation between the maximum values of ε^* obtained through Eq. 1 and the experimental grain sizes is graphically shown in Fig. 5. The resulting points were fitted by a third degree polynomial.

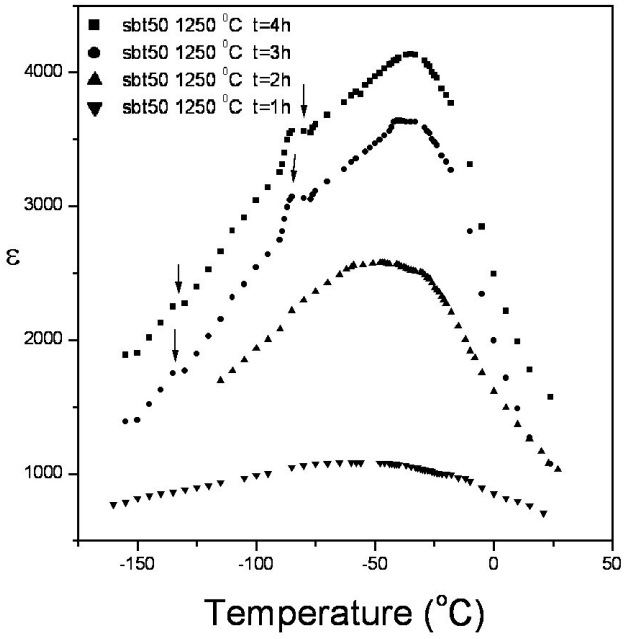

FIGURE 4. Temperature dependence of the dielectric permittivity with temperature measured at 1 kHz.

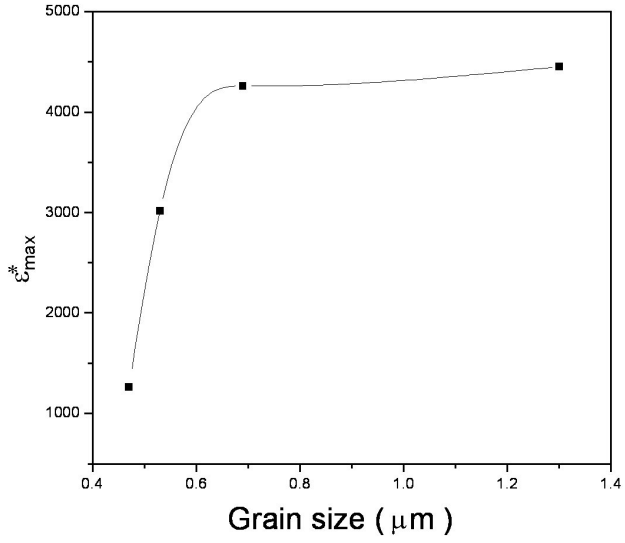

FIGURE 5. Maximum values of the permittivity obtained from Eq. 1 plotted against grain size.

4. Grain Kinetics

The *transformed fraction* ω of sintered material is defined as the ratio between the partial areas and the total area under the fitted curve in Fig. 4. A description of the evolution of the sintering process focused on grain size may be performed based on the behavior of ω. Figure 6 shows the relation between ω and D to be a sigmoidal function which allows us to identify the sintering process as a heterogeneous phase transformation consisting of a nucleation and growth mechanisms.

Using the results obtained in this study, a fitting process was performed to verify the behavior shown in Fig. 6. At this point, it is convenient to use the Johnson-Mehl-Avrami equation, to interpret the experimental results:

$$\omega = 1 - exp(-kt^n). \tag{2}$$

Here, ω is the transformed fraction, k is a constant characteristic of the process and n is a number associated to the nucleation and growth mechanisms. For this purpose,

$$Ln\left[Ln\left(\frac{1}{1-\omega}\right)\right]$$

Vs Ln(t) was plotted and the result is presented in Fig. 7. A value of 3 was determined for the slope of the curve and

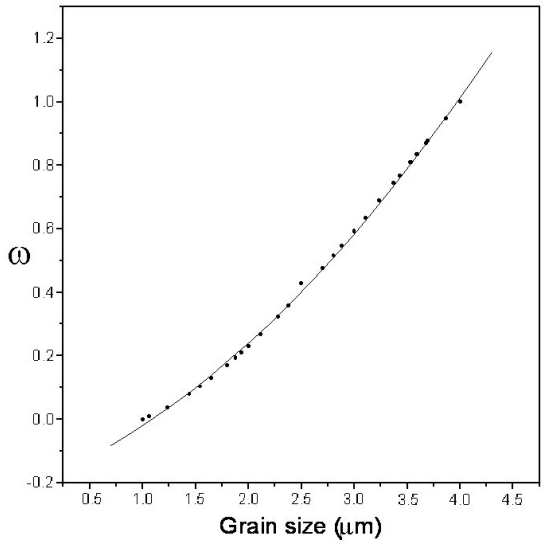

FIGURE 6. The transformed fraction ω as a function of grain size.

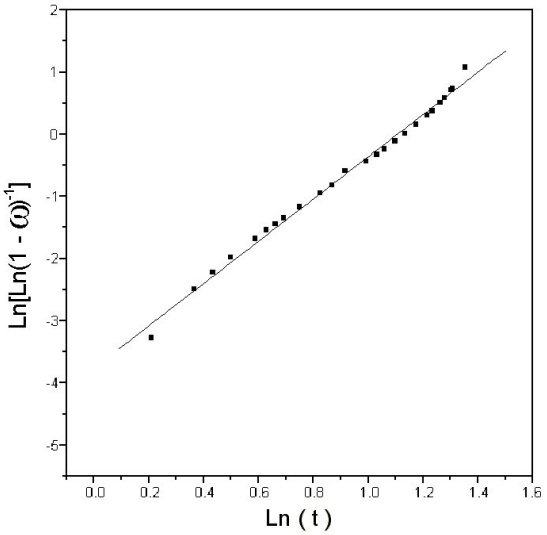

FIGURE 7. A plot of Ln[Ln(1/ 1-ω)] vs Ln(t) to determine the value of n in the Johnson-Mehl–Avrami equation.

corresponds to the value of the exponent n of the Johnson-Mehl-Avrami equation, therefore, according to Cahn and Haansen [9], the nucleation rate is zero, that is, all the nuclei were already present at the initial state and from there, the grain grows linearly. This conclusion is in excellent agreement with the results shown in Fig. 3.

5. Conclusions

From dielectric measurements at 1 kHz and scanning electron microscopy performed on $Sr_{0,5}Ba_{0,5}TiO_3$ samples a dependence of the grain size on the sintering time is experimentally determined. The Johnson-Mehl–Avrami equation is successfully used to interpret the experimental results. Starting from a fixed initial nuclei distribution, the linear behavior of the grain size with the sintering time found in the experiment is correctly described.

Acknowledgments

This work was partially sponsored by CoNaCyT Proj. No. 26314E DGAPA Proj. No. IN115098. We thank I. Gradilla, G. Soto and E. Aparicio for their technical help. S. García thanks DGIA-UNAM for its financial support.

1. I. Kingon, S.K. Streiffer, C. Basceri, and S.R. Summerfelt, *MRS Bulletin* **21** (1996) 46.
2. J.M. Siqueiros *et al.*, *Rev. Mex. Fís.* **46** (2000) 113.
3. O. Tikhomirov, H. Jiang, and J. Levy, *Appl. Phys. Lett.* **77** (2000) 2048.
4. l. Boarasu, L. Pintilio, and M. Kosec, *Appl. Phys. Lett* **77** (2000) 2231.
5. N. Ichinose and T.Ogiwara, *Jpn. J. Appl. Phys.* **34** (1995) 5198.
6. S. Zafar *et al.*, *Mat. Res. Soc. Symp. Proc.* **493** (1998) 15.
7. C.Hubert *et al.*, *Mat. Res. Symp. Pro.* **493** (1998) 69.
8. L. Zhang, W.L. Zhong, and L.C. Wang, *Solid State Commun.* **107** (1998) 769.
9. S. Nomura, *J. Japn. Phy. Soc.* **11** (1995) 924.

10. H-Y Chang, K-S Liu, and I-N Lin, *J. Europ. Ceram. Soc.* **16** (1996) 63.

11. G. Arlt, *Ferroelectrics* **104** (1990) 217.

12. F.D.Morrison, D.C. Sinclair, and A.R. West, *J. Appl. Phys.* **86** (1999) 6355.

13. S-H, Kim, H-W. Seon, J-G. Park, J-H. Park, and Y. Kim, *Jpn. J. Appl. Phys.* **38** (1999) 4818.

14. Y. Sato, H.Kanai, and Y. Yamashita, *Jpn. J. Appl. Phys.* **33** (1994) 1380.

15. G. Arlt, *J. Appl. Phys.* **58** (1985) 1619.

16. F. Wang *et al.*, *J. Mat. Res.* **13** (1998) 1243.

17. E.M. Lines and M. A. Glass (Clarendon Press, Oxford, 1977).

18. D.W. Kingery, K.H. Bowen, and R.D. Uhlmann (John Wiley & Sons, New York, 1976).

19. R.W. Cahn and P. Haansen, *Physical Metallurgy*, 4^{th} Edition. Vol 2 (North Holland. Amsterdam, 1996).

20. J. Portelles, *Obtención y Caracterización de Cerámicas con Transición de Fase Difusa*, PhD Thesis, Facultad de Física, Universidad de La Habana, (1994).

21. Landolt-Bornstein, "*Numerical Data and Functional Relationships in Science and Technology*", Vol. 16, Ferroelectrics and Related Substances, Subvolume a: Oxides, T. Mitsui, S. Nomura. Editors K.-H. Hellwege and A. M. Hellwege, (Springer-Verlag Berlin, Heildelberg, New York, 1981).

22. D. Payne and E.L. Cross, *Ceramic Microstructures* (M.R. Fulrath and A.J. Park, Westview Press, 1977).